

# ANALYSIS OF THE LONG-TERM AREA-TO-MASS RATIO VARIATION OF SPACE DEBRIS

**J. Herzog**

*Astronomical Institute, University of Bern,  
Sidlerstr. 5, CH-3027 Berne, Switzerland*

**T. Schildknecht**

*Astronomical Institute, University of Bern,  
Sidlerstr. 5, CH-3027 Berne, Switzerland*

## ABSTRACT

The internal catalogue of space debris objects maintained by the Astronomical Institute of the University of Bern (AIUB), contains many objects with observations over long time spans. They are observed regularly with ESA's 1-meter telescopes in Tenerife (Spain), AIUB's 1-meter telescope ZIMLAT and 30-centimeter telescope ZimSMART in Zimmerwald near Bern (Switzerland).

We analysed Area-to-Mass ratio (AMR) variations of 17 objects for which observations covering a time span of approximately one year or more were available. The median AMR values ranges from  $0.005 \text{ m}^2 \text{ kg}^{-1}$  to  $45 \text{ m}^2 \text{ kg}^{-1}$ . The class of Low Area-to-Mass ratio objects (LAMR) with AMR values lower than  $1 \text{ m}^2 \text{ kg}^{-1}$  is covered as well as the class of High Area-to-Mass ratio objects (HAMR).

Although the observations were post-processed, the same approach as in the routine processing was used: observation arcs as long as possible are fit with a constant AMR value. As a consequence, the AMR values are averaged over these intervals. Also, the individual arc lengths are varying and intervals are overlapping, because observations used in previous orbit determinations are used again. If adding results in poor fits, the oldest observations are taken off until the requirements for a "good" orbit are fulfilled. The procedure acts as a low-pass filter and only AMR value variations with low frequencies may be determined.

For this small sample, we categorised the objects according to the features visible in the development of the AMR values over time. The classes are applicable to both, LAMR and HAMR objects.

## 1. AREA-TO-MASS RATIO OF SPACE DEBRIS

The area-to-mass ratio (AMR) is a parameter to categorise space debris objects, furthermore, it is an additional parameter in an orbit determination. Compact, satellite-like objects have AMR values of  $1 \text{ m}^2 \text{ kg}^{-1}$  and less (low area-to-mass ratio objects, LAMR); large and/or very light, foil-like objects have AMR values of more than  $1 \text{ m}^2 \text{ kg}^{-1}$  (high area-to-mass ratio objects, HAMR). The latter objects have a large surface area, which is exposed to the radiation of the Sun, compared to their mass. Their orbits are highly influenced by the Solar radiation pressure. The orbital elements show characteristic variations (see [1] and [2]).

The surface exposed to the Sun is changing for rotating objects and one expects a change of AMR values over time. With the tool *CelMech*, developed by G. Beutler (see [3]), an average AMR value is estimated for the complete arc used in the orbit determination. When using arcs as long as possible, one obtains information about the long-term behaviour of the AMR value for each object.

In this study, we analysed objects of the Geostationary Ring with median AMR values between  $0.006 \text{ m}^2 \text{ kg}^{-1}$  and  $45 \text{ m}^2 \text{ kg}^{-1}$  and cover the LAMR as well as the HAMR objects.

## 2. ORBIT DETERMINATION

Each orbit determination was performed with the longest arc of observations, which fulfilled the criteria of a “good” orbit. One criterion is the RMS of the residuals of the fitted orbit with respect to the observations. The AIUB internal limit of the RMS is less than  $2''$  for an orbit to be considered as “good”. The estimated uncertainty of the scaling factor for the Solar radiation pressure had to be smaller than 20 % of the scaling factor itself. Consequently, the computed AMR value of that orbit also carried a small uncertainty.

Observations of a subsequent night were added and another orbit determination was performed. If the orbit determination was successful the orbit was stored into the data base. Otherwise, the oldest observations were excluded from the used arc until the orbit could be considered to be “good” again.

The orbital elements from the preceding orbit determination are used as a priori elements for the latest orbit determination.

The individual AMR values are averaged over the interval covered by the used arc. As some observations are also used in the following orbit determination with new observations, the individual AMR values are not independent from each other. The median AMR value is then the median of the AMR values from each orbit determination of an object. Furthermore, for a rotating object, which surface exposed to the Sun varies with time, a median AMR might only be a snap-shot.

This procedure is applied to the routine processing of the AIUB when obtaining new observations.

## 3. THE DATA SET

We selected 17 objects of the AIUB internal catalogue with median AMR values between  $0.006 \text{ m}^2 \text{ kg}^{-1}$  and  $45 \text{ m}^2 \text{ kg}^{-1}$ , consisting of seven LAMR and 10 HAMR objects. This is a subset of the complete catalogue with 243 LAMR and 97 HAMR objects (as of June 2012). We will present the results of four of the objects in detail, which are representative for the other objects.

Tab. 1 shows the objects with their median AMR value. In the last column, there is the characterisation in individual object classes of the AMR values over time.

We defined criteria in order to categorise objects based on the variation of AMR values over time. For the distribution of all AMR values we determined the median value and the standard deviation ( $1-\sigma$ ). A ‘peak’ in the graph is defined as an AMR value, which is at least three times the standard deviation ( $3-\sigma$ ) above or below the median. If a graph shows variation but no peaks and the variation does not exceed 5 % peak-to-peak, it is called ‘flat’. For rotating and tumbling space debris objects it is unlikely that they show this behaviour, but nearly spherical objects like crumpled foil might fulfil the condition even when rotating.

If the variation exceed 5 % peak-to-peak, but still no dominant peak is visible, we classify as ‘variation’ (class ①). If at least one dominant peak, according to the definition above, exists, we set three categories:

peaking to higher AMR values (‘high peak’, class ②), to lower AMR values (‘low peak’, class ③), and in both directions (‘high and low peaks’, class ④), respectively.

In the subset we analysed for this study, there are no objects, which would fall into the category of flat AMR curves. The AMR value variation always exceeds 5% peak-to-peak.

Tab. 1. Objects of this study with their median AMR value and classification

	class object	median AMR value	class feature(s)
①	EGEO32	1.70	variation
②	05049E	0.074	high peak
③	EGEO39	4.0	low peak
④	S95300	28.58	high and low peaks

Of course, the list of criteria is not complete, e. g. no statement concerning periodic behaviour of the peaks or secular trends is included. Also, the selection of objects may not be representative as they were primarily chosen to have many observations over a large time span.

#### 4. RESULTS

The selected objects were analysed like in the routine processing of AIUB, although it was a post-processing. This means, that the used observation arcs were as long as possible for each orbit determination.

The results of the representative objects are shown in Fig. 1. The red line represents the median AMR value of the distributions. The green lines are the  $3\text{-}\sigma$  upper and lower limits to define peaks.

##### EGEO32

A variation of the AMR values is visible, especially there are two high peaks (at 53880 and 54080, respectively) and a low peak around 54180. But no AMR value exceeds the  $3\text{-}\sigma$  limit, displayed by the green lines (see Fig. 1(a)). The peak heights are  $2.35\sigma$  above and  $-2.35\sigma$  below the median AMR value. It is therefore the representative object of the ‘variation’ class ①.

The first peak nearly reaches the upper limit, while the last peak nearly reaches the lower limit. Unfortunately, the observations ended and the minimum might not be already reached. No statement concerning periodicity can be made.

In the analysed subset of the AIUB internal catalogue, there are four objects falling in this category. Tab. 2 summarises the AMR characteristics of the objects of this class, together with the total arc lengths in days and the number of performed orbit determinations (OD), which represents the data points in the graphs. The median AMR values and the variation peak-to-peak in percent are shown in the last columns. Although the peak-to-peak variation is large for some objects (e. g. 132% for 05049F) or peaks are visible (see Fig. 1(a)), respectively, the peaks were always below the  $3\text{-}\sigma$  limit. Therefore, they are put into this class.

Tab. 2. Objects of class ①

Object	Total arc length (d)	Number of OD	Median AMR value ( $\text{m}^2 \text{kg}^{-1}$ )	peak-to-peak variation (%)
EGEO32	417	27	1.70	28
05049F	619	30	0.065	132
E07311D	1217	71	1.378	30
Z11096L	378	12	0.020	63

### 05049E

The AMR values show variation over the entire analysis interval (see Fig. 1(b)). One dominant peak is visible around MJD = 54313. This peak exceeds the  $3\text{-}\sigma$  limit with  $4.28\sigma$  above the median AMR value, which makes this object the representative object of the ‘high peak’ class ②.

Here again, five objects of the subset fall in this category, shown in Tab. 3. There, beside the object names, the number of performed orbit determinations, their total arc length, their median AMR value and the height of their highest peak are given. The peak height is in units of the standard deviation of the AMR value distribution.

Tab. 3. Objects of class ②

Object	Total arc length (d)	Number of OD	Median AMR value ( $\text{m}^2 \text{kg}^{-1}$ )	peak height ( $\sigma$ )
05049E	2334	129	0.074	4.28
E03174A	2983	124	0.0067	7.33
E06321D	2001	174	2.5119	5.02
EGEO07	292	35	1.980	5.69
Z08343R	1256	41	0.0057	12.15

### EGEO39

The AMR values of this object are spread widely, the variation is more than  $5.1 \text{ m}^2 \text{ kg}^{-1}$  between minimum and maximum. The standard deviation  $\sigma$  is approximately  $0.9 \text{ m}^2 \text{ kg}^{-1}$ , which is 23.8% of the median value. This is the object with the largest variation in Fig. 1. The minimum falls below the  $3\text{-}\sigma$  limit, being  $-3.75\sigma$  below the median AMR value (see Fig. 1(c)). The object becomes the representative of the ‘low peak’ class ③. Unfortunately, the observations ended before the maximum value of the last peak might have been reached. Additionally, the observation period is short compared to the other representative objects, it was chosen because of its large range of AMR values.

From the analysed subset, six objects belong to this class. The objects of this class are shown in Tab. 4, together with the total arc lengths, the number of performed orbit determinations, median AMR values and the peak heights of the largest peak. The peak height is again in units of the standard deviation of the AMR value distribution and the minus sign denotes that the peak is lower than the median AMR value.

Tab. 4. Objects of class ③

Object	Total arc length (d)	Number of OD	Median AMR value ( $\text{m}^2 \text{kg}^{-1}$ )	peak height ( $\sigma$ )
EGEO39	130	34	4.0	-3.75
E07047A	1162	68	4.793	-6.21
E07308B	334	49	8.863	-6.26
E09293A	499	30	4.252	-3.97
E09325A	290	32	45.03	-3.34
Z09338F	881	212	0.0263	-3.04

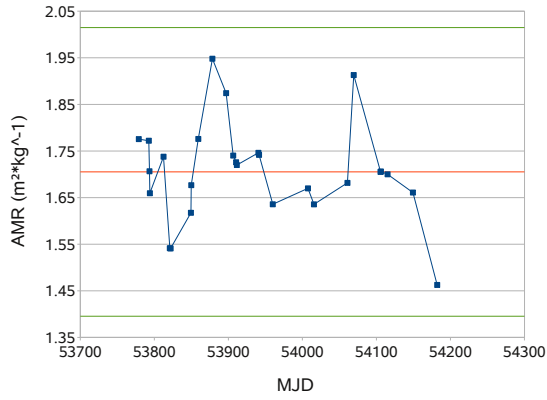
### S95300

This objects shows two peaks, a low peak at the beginning and a high peak near the end of the observations (see Fig. 1(d)). Both peaks exceed the  $3\text{-}\sigma$  limit, though the minimum of the first peak is not visible. The low peak is  $-4.43\sigma$  below the median AMR value, the high peak is  $4.74\sigma$  above it. This object is the representative for the ‘high and low peaks’ class ④.

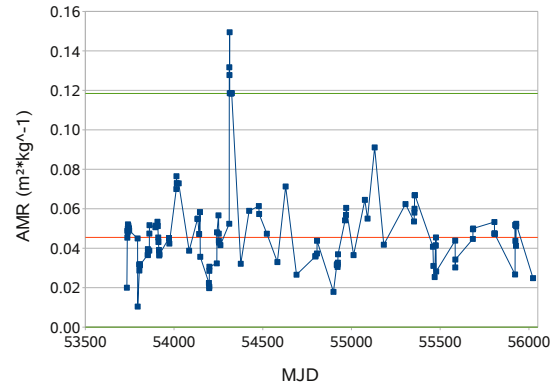
Two of the objects analysed fall into this class, shown in Tab. 5. Besides the object names, the total arc lengths, number of performed orbit determinations, the median AMR values and the peak heights are displayed. Again, the peak heights are given in units of the standard deviation of the AMR value distribution. Positive values denote peaks larger than the median AMR value, negative values denote peaks below the median AMR value.

Tab. 5. Objects of class ④

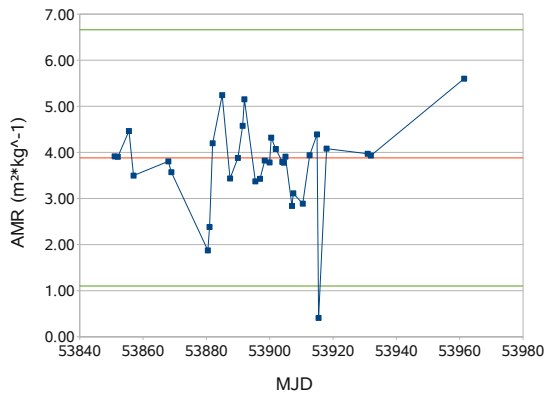
Object	Total arc length (d)	Number of OD	Median AMR value ( $\text{m}^2 \text{kg}^{-1}$ )	peak heights ( $\sigma$ )
S95300	406	66	28.58	-4.43 4.74
E06327E	1859	120	0.577	-4.53 4.42



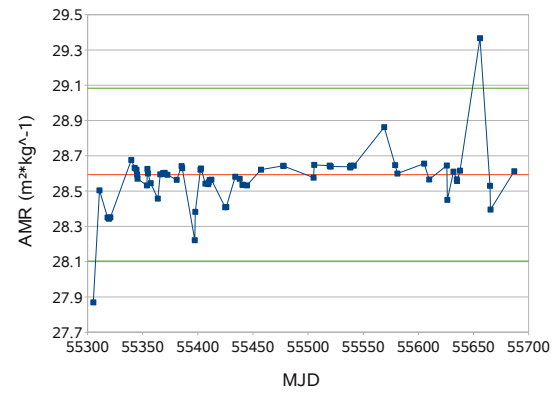
(a) 'variation' – EGEO32



(b) 'high peak' – 05049E



(c) 'low peak' – EGEO39



(d) 'high and low peaks' – S95300

Fig. 1. AMR values as a function of time of the four representative objects of this study; red line: median AMR value; green lines:  $3\text{-}\sigma$  upper and lower limit

## 5. CONCLUSIONS

We analysed the long-term behaviour of AMR values for objects in the AIUB internal object catalogue. The objects were classified according to significant structures in the AMR value variation over time. We defined four classes. The AMR values of objects in the first class show only variation without significant peaks. The AMR values of the objects of the other classes show peaks. We defined three classes with peaks: ‘high peaks’, ‘low peaks’ or with both kinds, respectively.

We selected 17 objects from the AIUB internal catalogue and determined orbits with estimating the AMR value. Based on the criteria defining the classes, we assigned them into the different classes. From the subset, the AMR values of four objects showed variation but no dominant peak. Five objects showed at least one dominant high peak, while six others showed at least one low peak. The last two objects showed high and low peaks.

The list of criteria is not complete, e. g. no statement about periodicity or secular trends could be made. Objects, whose AMR values do not show any variation and could be called flat, were not found in the subset. Also, the subset of objects and the relative abundance in the four classes might not be representative for the complete AIUB internal catalogue.

## 6. ACKNOWLEDGEMENTS

The work of Johannes Herzog was supported by the Swiss National Science Foundation through grants 200020–122070 and 200020–137934. The observations from the ESASDT were acquired under ESA/ESOC contracts.

## 7. REFERENCES

- [1] Reto Musci et al. Analyzing long observation arcs for objects with high area-to-mass ratios in geostationary orbits. *Acta Astronautica*, (66):693–703, 2010.
- [2] Carolin Früh. *Identification of Space Debris*. Shaker Verlag, 2011.
- [3] Gerhard Beutler. *Methods of Celestial Mechanics*. Springer-Verlag, Heidelberg, 2005.